Quantitative trait loci modulate neutrophil infiltration in the liver during LPS-induced inflammation

LYDIA E. MATESIC, EMILY L. NIEMITZ, ANTONIO DE MAIO,* AND ROGER H. REEVES[1]

Department of Physiology and *Division of Pediatric Surgery, The Johns Hopkins School of Medicine, Baltimore, Maryland 21205, USA

ABSTRACT **A crucial aspect of the inflammatory response is the recruitment of activated neutrophils (PMN) to the site of damage. Lytic enzymes and oxygen radicals released by PMN are important in clearing an infection or cellular debris, but can also produce host tissue damage. Failure to properly regulate the inflammatory response contributes to a variety of human diseases like sepsis and multiple organ dysfunction syndrome, the leading cause of morbidity and mortality in surgical intensive care units. Many aspects of human disease pathology, including hepatic PMN infiltration, can be recapitulated in mice using an endotoxic shock model. Six quantitative trait loci that predispose to high infiltration of PMN in hepatic sinusoids after high-dose endotoxin administration were provisionally identified. Two of these loci, *Hpi1* and *Hpi2* on mouse chromosomes 5 and 13, were mapped to the significant and highly significant level using a low-resolution genome scan on 122 intercross animals. These loci interact epistatically to produce a high degree of PMN infiltration. Intercross and recombinant inbred strain mice with a specific genotype at these loci always had a high infiltration response, indicating that genotype analysis at just these two loci can accurately predict a high PMN infiltration response. Genetic predisposition to the degree of PMN infiltration in the inflammatory response in mice suggests that analogous genetic mechanisms occur in human beings that could be used for diagnostic purposes.—Matesic, L. E., Niemitz, E. L., De Maio, A., Reeves, R. H. Quantitative trait loci modulate neutrophil infiltration in the liver during LPS-induced inflammation. *FASEB J.* 14, 2247–2254 (2000)**

Key Words: mapping · quantitative trait loci · inbred strains (A/J and C57BL/6J) · sepsis · multiple organ dysfunction syndrome

SEPTIC SYNDROME AFFECTS more than 175,000 people per year in the United States alone (1) and is characterized clinically by a hypermetabolic state that arises as a consequence of an exaggerated host inflammatory response to infection or to severe injury (2, 3). One detrimental consequence of sepsis is the development of multiple organ dysfunction syndrome (MODS), the leading cause of morbidity and mortality in intensive care units (4). Despite improvements in the care of critically ill patients during the past two decades, mortality rates from sepsis and MODS remain unchanged. Development of better therapeutic strategies requires a comprehensive understanding of the pathophysiological mechanisms underlying these disorders, particularly that of the inflammatory response.

The inflammatory response is characterized by a complex cascade of cellular changes including the activation of phagocytic cells, secretion of cytokines such as tumor necrosis factor (TNF) and interleukins (IL) 1, 6, and 8, and the expression of cell surface receptors like ICAM-1 on activated endothelial cells that guide the adhesion and extravasation of polymorphonuclear leukocytes (PMN) (5). In addition, different organ systems respond to these changes by expressing various groups of genes such as the IL-1- and IL-6-induced production of acute-phase proteins in the liver. Although these events are beneficial to the individual in the early stages of injury, an exaggerated or uncontrolled response can be detrimental. Under these circumstances, the infiltration of PMN in major organ systems like the lung and liver may result in secondary organ damage due to the release of lytic enzymes and oxygen radicals (6).

The genetic background of an affected individual may be an important component in the regulation of inflammation. Epidemiological studies have demonstrated that a familial clustering of susceptibility to infectious agents to chronic inflammatory diseases, and to autoimmune disease is due, in part, to genetic factors (7, 8). Polymorphic variants in the human *TNF* α and β loci that produce higher amounts of circulating TNF have been associated with higher mortality rates after severe sepsis (9). A polymorphism in the *IL1RA* gene that results in high levels of

[1] Correspondence: Biophysics 203, The Johns Hopkins University School of Medicine, 725 N. Wolfe St., Baltimore, MD 21205, USA. E-mail: rreeves@welch.jhu.edu

IL-1 receptor antagonist protein is a marker of susceptibility to sepsis (10).

Studies performed in animal models support the assertion that there is a genetic contribution to the inflammatory response. Differences in the systemic inflammatory response to lipopolysaccharide (LPS) administration among inbred strains of mice are well documented. Extensive analyses have focused on LPS hyporesponsive C3H/HeJ and C57BL/10SCr mice. It was recently discovered that these mice have a mutation in the toll-like receptor 4 (*Tlr4*) gene, a signal-transducing component of the cellular response to LPS (11, 12). Other inbred strains also show defects in certain aspects of the LPS-response, but do not have mutations in *Tlr4*. For example, A/J mice were found to be resistant to LPS-induced mortality at dosages where C57BL/6J (B6) mice were susceptible, and these observations were correlated with differences in the inflammatory response including the level of circulating TNF-α, IL-1β, IL-6, and the expression of acute-phase proteins in the liver (13). The degree of infiltrating leukocytes in the liver and lung also differs between these strains after administration of LPS (14). Several loci that control differential LPS-induced proliferation of cultured splenocytes derived from A/J or B6 mice were mapped in recombinant inbred (RI) and congenic strains (15).

Intraperitoneal (i.p.) administration of LPS results in greater hepatic PMN infiltration and ensuing necrosis in B6 than in A/J mice (**Fig. 1**), and this difference is highly significant (14). F_1 offspring from a cross between a B6 female and an A/J male ($B6AF_1$ mice) or from a cross between an A/J female and a B6 male ($AB6F_1$ mice) show a PMN infiltration profile similar to B6 mice, indicating that genes substantially contributing to this phenotype are neither sex linked nor imprinted. To map genes that predispose to high or low levels of endotoxin-induced hepatic PMN infiltration, linkage analysis was performed using the AXB/BXA RI strain set, and a low-resolution genome scan using 76 polymorphic markers evenly spaced throughout the genome were used on a panel of 122 intercross animals.

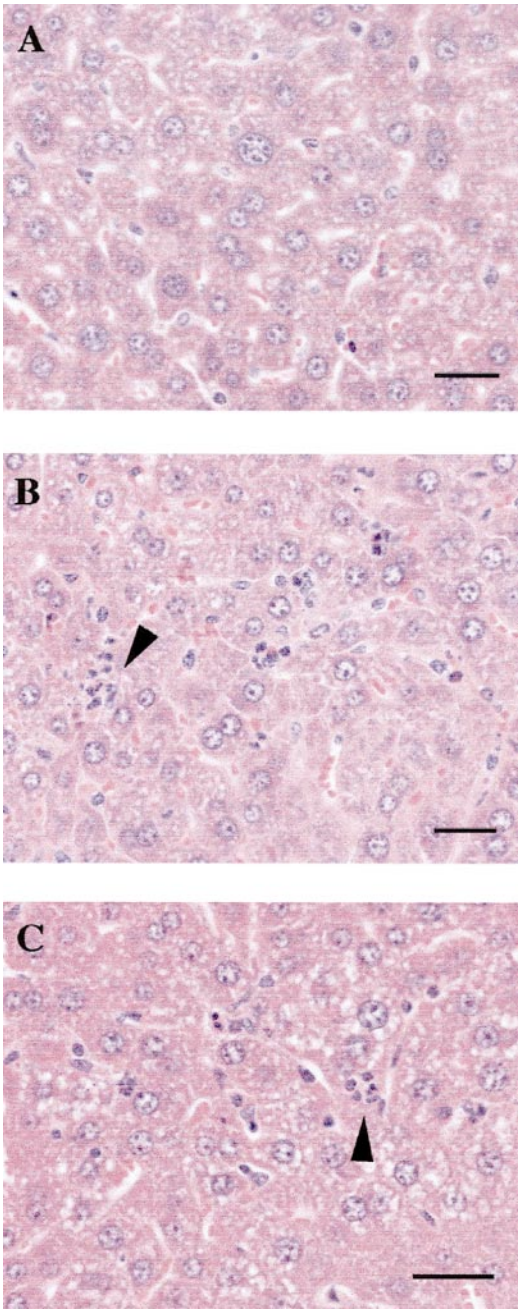

Figure 1. Treatment with endotoxin results in a higher frequency of hepatic PMN infiltration in B6 than in A/J mice. Histological sections of liver taken 24 h after LPS injection reflect the low number of infiltrating PMN in A/J relative to B6 and reciprocal F_1 mice. *A)* A/J; *B)* B6; *C)* [A/J × B6]F_1. Arrowheads indicate PMN in hepatic sinusoids. Bar is 100 μm.

MATERIALS AND METHODS

Animals

A/J, A/WySnJ, C57BL/6J, C57BL/10SnJ, $B6AF_1$, C57BL/6J-*Il6*^{tm1Kopf}, B10.A-*H2*^{a}-*H2-T18*^{a}/SgSnJ, A.BY-*H2*^{b}-*H2-T18*^{b}/SnJ, and AXB/BXA RI strains were obtained from the Jackson Laboratory (Bar Harbor, Maine) at 6–7 wk of age. Female A/J mice were bred to B6 males to produce $AB6F_1$ offspring. Two intercrosses were created. The first was derived from a cross between male and female $AB6F_1$ mice and yielded 15 male progeny. The larger intercross (between two B6A F_1 mice) produced 107 male progeny. No phenotypic differences were observed between these progeny sets, and all 122 animals were used for analysis. Intercross progeny were weaned at 3–4 wk of age, separated by sex, and maintained until they reached the appropriate age for experimentation. All animals were housed in microisolators in an antigen- and virus-free room from the time of receipt or of weaning until they were 8–9 wk of age. Only male mice were phenotyped in this study.

Phenotyping

Male mice, 8–9 wk of age, were injected i.p. with 15 mg/kg of LPS derived from *Escherichia coli* O26:B6 (Difco, Detroit,

Mich.; manufacturer's LD_{50}=12.53 mg/kg) resuspended in 0.9% NaCl (Abbott, Abbott Park, Ill.). Animals were killed by cervical dislocation 24 h postinjection. Livers were removed and fixed in 10% neutral buffered formalin. After being mechanically rinsed, dehydrated, and embedded in paraffin, the tissue was sectioned (5 μm) and stained with hematoxylin and eosin. Neutrophil infiltration was quantified by counting the number of PMN in 10 high-power fields (h.p.f.; 400× magnification). Only fields that were 90–95% liver parenchyma with nonfocal necrosis were selected. The average number of PMN from the 10 fields was the infiltration score for that animal. When slides from 20 animals were blinded and recounted by the same investigator, the average difference in infiltration score was found to be 3.35 where the mean score was 34 ± 17.5. All experimental procedures were carried out in accordance with protocols approved by the Johns Hopkins School of Medicine Animal Care and Use Committee and in conformance with guidelines established in the National Research Council's *Guide to the Care and Use of Laboratory Animals.*

Genotyping

DNA was extracted from tails of intercross progeny by salting-out as described (16). PCR was carried out using 100 ng of template DNA. Primers for simple sequence length polymorphisms (SSLP) that differ between A/J and B6 progenitor strains were purchased from Research Genetics (Huntsville, Ala.) and used as suggested by the manufacturer.

Linkage analysis

Linkage analysis was performed using Map Manager QT, v28 (17). For RI strains, infiltration scores from three animals were averaged and entered as quantitative trait loci (QTL). These were compared against the AXB/BXA set for QTL mapping (18). Linkage and % variance accounted for by a QTL was detected for the intercross set by comparing the infiltration scores of 122 progeny to the genotypes of those animals at 76 loci throughout the genome. Suggestive, significant, and highly significant threshold levels were determined by the permutation test function of Map Manager, which is based in the statistical methods developed by Churchill and Doerge (19). A likelihood ratio statistic (LRS) value of 4.6 is equivalent to one LOD. A two-LOD support interval was determined for significant loci as the region at which the LRS value was within 9.2 units (two LOD units) of the peak value.

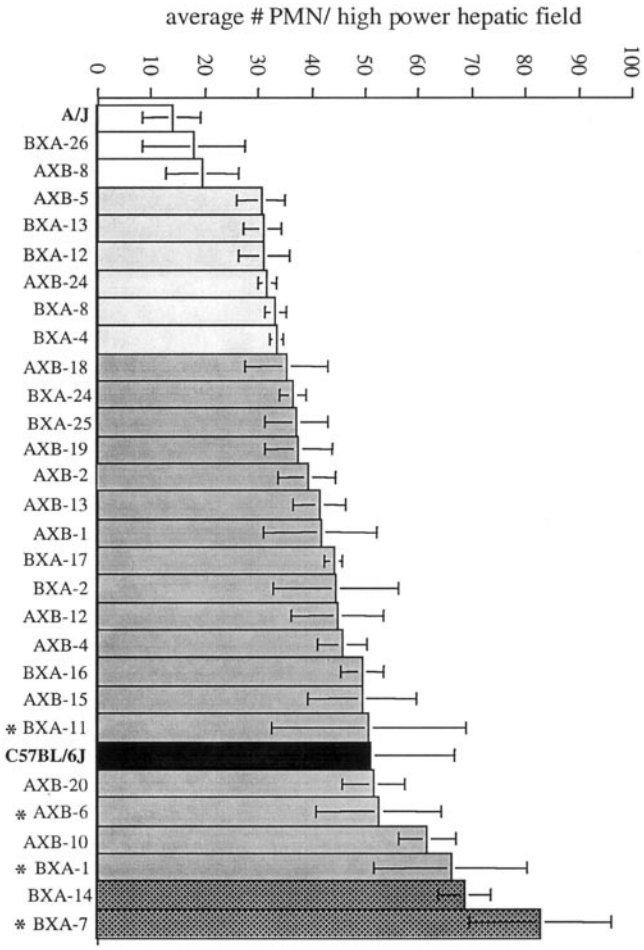

Figure 2. Hepatic PMN infiltration phenotypes of AXB/BXA RI strains. Three males from each of 28 AXB/BXA RI strains were tested for hepatic PMN infiltration in response to LPS. Two RI strains (white) showed a phenotype that was not significantly different from that of the A/J founder; the remaining 25 strains had a high infiltration response like the B6 founder (shaded). Those shaded in light gray have infiltration scores one standard deviation less than that of the B6 average. Infiltration scores of those strains shaded gray are within one standard deviation of the B6 average, whereas stippled bars indicate infiltration scores one standard deviation greater than the B6 average. The phenotypes of these strains form a continuous distribution, consistent with a complex trait. Strains indicated by an asterisk are homozygous for the B6 allele at both *Hpi1* and *Hpi2*.

RESULTS

Linkage analysis

Three males from 28 AXB/BXA RI strains were assessed for hepatic PMN infiltration after LPS treatment. The phenotypes of these strains form a continuous distribution, consistent with a quantitative trait (**Fig. 2**). The average infiltration score (PMN per h.p.f.) from each RI strain was entered into Map Manager QT (17) as a quantitative trait, and linkage was evaluated against the edited AXB/BXA data set (18). Suggestive linkage was detected at four loci. SSLP marker *D5Mit13* had the highest LRS, a measure of linkage. The LRS score for this locus was 9.6, where 7.6 is suggestive and 12.8 is significant. The other markers that showed suggestive linkage in this data set were *D6Mit50*, *D9Mit16*, and a restriction fragment length polymorphism in the *Tnf* gene that served as a marker on mouse chromosome (Chr) 17.

The relatively low statistical confidence in linkage yielded by the RI analysis reflects, in part, the limited number of meioses represented in RI sets. Although these results do not prove linkage, they do suggest areas of the genome that should be investigated in greater detail. Further examination of genes that contribute to the differential PMN infiltration in B6 and A/J mice were pursued by mapping in 122 intercross animals (244 meioses). The infiltration

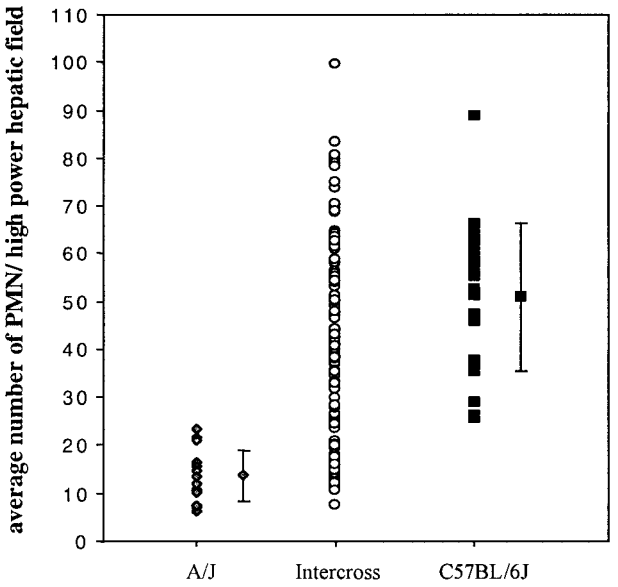

Figure 3. LPS-induced hepatic PMN infiltration in intercross progeny form a continuous distribution across the entire range of A/J and B6 responses. Livers from A/J, B6, and 122 male progeny of an intercross between these strains were isolated and fixed 24 h after i.p. injection of LPS (15 mg/kg). Infiltration scores for each animal were determined by averaging the number of PMN in 10 high-power hepatic fields (400×). No overlap was seen between 15 A/J and 21 B6 animals, and the mean infiltration scores for these strains is significantly different ($P<10^{-5}$). Mean ± standard deviation for A/J and B6 are indicated.

scores for these animals were distributed continuously from 7 to 100, consistent with a quantitative trait (**Fig. 3**). Genotypes at 76 loci were determined in the intercross progeny (**Fig. 4**). Assuming a mouse genome length of 1500 cM, these 76 markers occur, on average, every 20 cM. Therefore, any contributing QTL is no more than 10 cM from the closest typed marker. Only one marker was typed on the X chromosome because F_1 data suggested that major contributors are not sex linked (14). Analysis of linkage using Map Manager QT (17) detected significant linkage at marker *D13Mit17* on Chr 13 and suggestive linkage with markers *D1Mit318*, *D5Mit13*, *D5Mit197*, *D8Mit80*, *D9Mit352*, and *D16Mit181* (Fig. 4).

Refinement of QTL map positions

Six additional Chr 13 SSLP markers that map near *D13Mit17* were typed to confirm this linkage. Also, five Chr 5 markers that map between *D5Mit13* and *D5Mit197* were typed since *D5Mit13* exhibited a suggestive linkage in both the intercross and RI analyses. These genotypes helped refine the localization of two contributing *Hpi* (*h*epatic *P*MN *i*nfiltration) QTL (**Fig. 5**). The linkage peak on Chr 13 was detected between markers *D13Mit236* and *D13Mit248*. The threshold value for 'highly significant' linkage corresponds to $P<0.001$ for the genome scan (20). The two-LOD support interval around *Hpi1* is defined as the region where the LRS score is within 9.2 units of the peak value (see Materials and Methods) and spans 15 cM. The *Hpi1* interval accounts for 16% of the total trait variance. Using a constrained recessive regression model, highly significant linkage ($P<0.001$) was detected at one of the added markers, *D13Mit88* (LRS=22.1).

The addition of markers on Chr 5 raised the suggestive LRS for this locus to a significant level (LRS=12.7) in the intercross analysis using either an additive or recessive model for regression. The two LOD support interval extends 34 cM from the proximal end of Chr 5. The peak LRS score was observed at *D5Mit233*. *Hpi2* accounts for 8% of the total trait variance. This data set also defines the best marker map order for four SSLP markers to be *D5Mit81-D5Mit233-D5Mit391-D5Mit394* rather than *D5Mit391-D5Mit81-D5Mit233-D5Mit394*, as reported in the composite Chr 5 map by Mouse Genome Informatics (http://www.jax.informatics.org).

Epistasis in predisposition to high PMN infiltration

The average infiltration scores seen in mice with each of the nine possible combinations of genotypes at *Hpi1* and *Hpi2* were compared to examine possible interactions between these loci. A homozygous B6 genotype (B/B) at *Hpi1* on Chr 13 was seen to contribute to a significantly higher overall infiltration score (**Table 1**, shaded cells), consistent with the

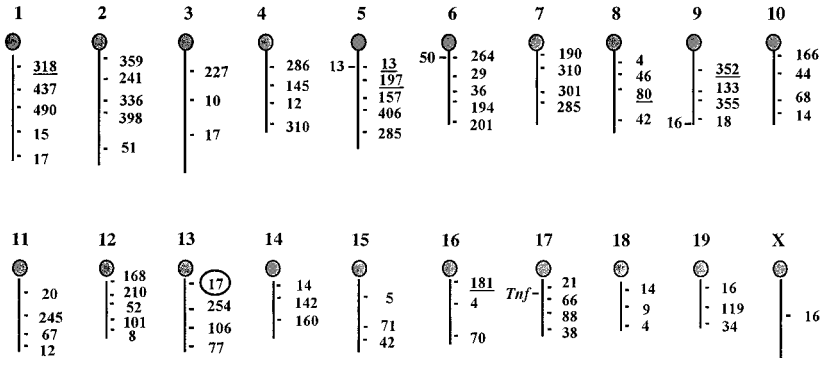

Figure 4. Polymorphic markers used in the low-resolution genome scan. Ideograms of 20 mouse chromosomes are depicted with the positions of 76 markers used in the genome scan shown to the right. Scale and map positions are based on the Mouse Genome Informatics consensus linkage maps (http://www.jax.org). All markers used (except *Tnf*) are SSLP markers and are abbreviated by the unique numerical identifier (e.g., *D5Mit13* is abbreviated as 13′ on Chr 5). Markers shown to the left of a chromosome showed suggestive linkage in the RI analysis. Underlined markers show suggestive linkage and circled markers show significant linkage in the initial genome scan.

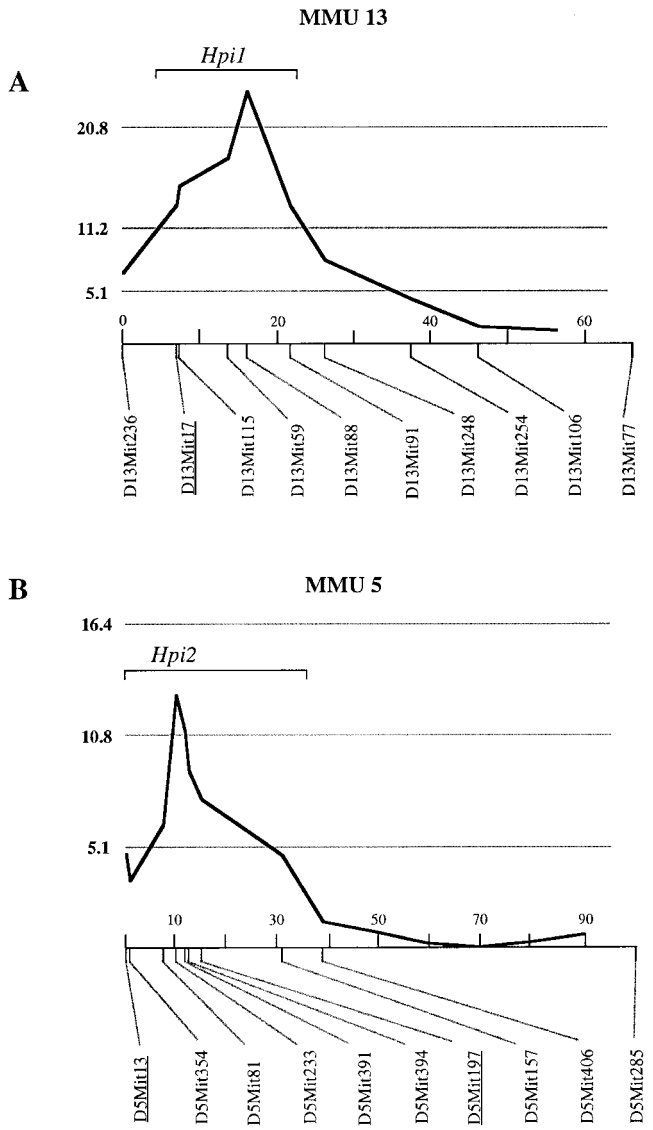

Figure 5. Interval mapping of *Hpi* QTL. The interval mapping function of Map Manager QT was used to map *Hpi1* and *Hpi2* after typing additional markers around these loci. *A)* Six additional markers that map in the vicinity of *D13Mit17* were typed in the intercross set progeny. These markers increase the peak LRS value to 22.1. The 2 LOD support interval spans 15 cM (bracket). *B)* Five additional markers that map between *D5Mit13* and *D5Mit197* were typed, raising the LRS for *Hpi2* to 12.7, above the threshold for significant linkage. The two LOD support interval of 34 cM is limited by the edge effect of the MMU 5 telomere. For each graph, the suggestive, significant, and highly significant threshold values are given. Marker order and map positions are calculated using the data from this cross. Markers that showed suggestive or significant linkage in the initial low-resolution genome scan are underlined.

recessive model that provided the strongest evidence for linkage at this locus. The high infiltration scores in *Hpi1* B/B animals were unaffected by either an A/A or A/B genotype at *Hpi2* on Chr 5, but the scores increased substantially (to an average of 69) when the *Hpi2* genotype was B/B. That is, the *Hpi2* genotype had no apparent effect on infiltration score in mice with any genotype at *Hpi1* other than B/B, and only a B/B genotype at *Hpi2* affected the phenotype in mice that were B/B at *Hpi1*. This epistatic interaction was also seen using the composite interval mapping function of Map Manager QT. When the analysis was run to control for the effect of *Hpi1*, linkage was no longer detected at *Hpi2*. In contrast, significant linkage was still detected at *Hpi1* when effects of a Chr 5 locus were controlled.

Simple inspection of genotypes showed that among the 122 intercross progeny, 9 of the 14 with the highest infiltration scores were homozygous for the B allele at both *Hpi1* and *Hpi2*. The lowest infiltration score seen in a double homozygous B6-type mouse was 33 PMN/h.p.f., more than three standard deviations higher than the A/J mean (13.8±5.3) and substantially higher than any A/J mouse in the study (Fig. 3). Intercross progeny with the lowest infiltration scores had a paucity of B6 alleles at *Hpi1* and showed the 1:2:1 distribution of genotypes at *Hpi2* expected for a locus with no involvement in the phenotype. There was no obvious 'protective' combination of genotypes at these two loci corresponding to the predisposition toward high PMN infiltration in B6-type double homozygous progeny (data not shown).

Candidate gene analysis

D5Mit13, the marker detected by both RI and intercross analysis, maps just distal to the gene encoding IL-6 (*Il6*), an important cytokine mediator of the inflammatory response. The contribution of *Il6* to the LPS-induced PMN infiltration response was evaluated in C57BL/6J-*Il6*tm1Kopf mice, which have a homozygous deletion of the *Il6* gene on a B6 background (21). Absence of *Il6* had no effect on LPS-induced PMN infiltration. Mean infiltration scores for five B6 and five C57BL/6J-*Il6*tm1Kopf were 43.5 ± 15.1 and 46.7 ± 13.9, respectively.

The region of suggestive linkage on Chr 17 determined by RI analysis includes the major histocompatibility complex, *H2*, and the proinflammatory cytokine *Tnf*. A/J and B6 mice are known to have allelic variants at the *Tnf* locus, which have been associated with different levels of TNF-α in several strains of mice (22, 23). The possible contribution to the infiltration phenotype of *H2*, *Tnf*, or another gene in this region of Chr 17 was assessed using congenic mice. The region of Chr 17 in B10.A-*H2*a-*H2-T18*a/SgSnJ congenic mice includes the *H2* complex and *Tnf* (22), and is derived from the inbred strain A/WySnJ, a low responder in the hepatic PMN infiltration assay like A/J. The remainder of the genome of this congenic strain is derived from C57BL/10SnJ, which demonstrated a high level of LPS-induced PMN infiltration like B6. These con-

TABLE 1. *Epistatic interaction of Hpi1 and Hpi2*[a]

		Genotype at Hpi2, chromosome 5			
		A/A	A/B	B/B	Totals
Genotype at *Hpi1*, chromosome 13	A/A	33.5 ± 4.6 (9)	35.6 ± 4.8 (12)	35.6 ± 6.9 (8)	35.0 ± 3.0
	A/B	28.9 ± 5.0 (11)	35.7 ± 3.0 (40)	37.8 ± 4.8 (11)	34.9 ± 2.3
	B/B[b]	42.5 ± 4.1 (2)	44.7 ± 5.3 (14)	69.9[c] ± 5.5 (11)	54.8 ± 4.3
	Totals	32.0 ± 3.2	37.6 ± 2.3	49.0 ± 4.3	39.5 ± 1.9

[a] Avg. number of PMN per h.p.f. ± SE are given for (n) animals of each genotype class. [b] Mice with a B/B genotype at Hpi1 showed significantly higher PMN infiltration values than other *Hpi1* genotypes ($P = 1.22 \times 10\text{-}4$, t test assuming unequal variance). [c] Mice with a B/B genotype at both Hpi1 and Hpi2 showed significantly higher PMN infiltration than other genotype classes ($P = 7.83 \times 10\text{-}5$, t test assuming unequal variance).

genic mice showed high PMN infiltration after LPS, suggesting that *H2* and *Tnf* are not pivotal to this response (**Table 2**). The PMN phenotype of the reciprocal congenics, A.BY-*H2*b-*H2-T18*b/SnJ, supports this conclusion. These mice have a B-derived MHC on an A background and show the low PMN infiltration response to LPS. Thus, allelic differences of genes that map within the MHC do not correlate with PMN infiltration phenotypes.

DISCUSSION

In human beings and other mammals, infiltration and sequestration of PMN in the liver and other organs is one of the hallmarks of a systemic inflammatory response induced by endotoxin and by other conditions such as ischemia/reperfusion, trauma, sepsis, or organ transplantation (24). The endotoxin-induced infiltration often results in liver damage, and this hepatotoxicity can be significantly reduced in experimental animal models if neutrophils are depleted before endotoxin is administered (25). Antibody therapies have been devised to reduce liver damage during a systemic inflammatory response. Most of these strategies try to eliminate the interaction between infiltrating PMN and endothelial cells (26–28) or the downstream effectors of the LPS signaling pathway (29). These preventative therapies against endotoxin-induced damage have been tested in animal models with varying success.

The mouse system provides a powerful tool for unraveling the complex interaction of genes and environment in the inflammatory response. Whereas an inflammatory response arises as a consequence of stochastic events in humans, the mouse system allows for controlled initiation of this response in animals of the same age that have been housed under identical pathogen-free conditions since birth. The use of inbred strains defines and limits the sources of genetic variation, providing a greatly simplified set of polymorphic alleles whose interactions are accordingly observed much more readily than in an outbred population. Genetic approaches using mouse are further facilitated by unique genetic tools such as RI strains, congenic strains, and mice with targeted mutations.

Two loci on Chr 5 and 13 that contribute to the differential PMN infiltration response in A/J and B6 mice were identified through RI mapping and a low-resolution genome scan of 122 intercross animals. The support intervals around QTL identified in this first level of mapping are broad and include too many candidate genes for a comprehensive mutation screen. On the other hand, the Chr 13 and Chr 5 2-LOD support intervals each exclude more than 97% of mouse genes as candidates. These significant linkages and the several suggestive linkages identified in the first stage analysis focus future mapping efforts using a high-resolution intercross panel (in progress). Candidate genes from the *Hpi1* and *Hpi2* loci with particular biological relevance to the PMN infiltration phenotype were assessed by examination of congenic and gene-targeted mice.

TABLE 2. *Assessment of the contribution of the MHC to the PMN infiltration phenotype*

Strain	n	*H2* allele	*Tnf* allele	Average PMN infiltration score ± standard deviation
A/WySnJ	5	A	A	13.2 ± 3.3
A.BY-*H2*[b]-*H2-T18*[b]/SnJ	5	B	B	16.3 ± 6.7
B10.A-*H2*[a]-*H2-T18*[a]/SgSnJ	5	A	A	68.9 ± 23.0
C57BL/10SnJ	5	B	B	85.0 ± 1.3

These tools rapidly and definitively eliminated these candidates, focusing interest on other genes in the target regions.

The demonstration in congenic strains that IL-6 is not involved in hepatic PMN recruitment after endotoxin exposure is interesting because it had been reported previously that IL-6 was associated with neutrophil recruitment and lung injury in hemorrhagic shock in mice (30), with PMN infiltration and ocular injury in endotoxin-induced uveitis in the rat (31) and with activation of leukocytes and severity of organ dysfunction in the systemic inflammatory response syndrome in humans (32). Our results show identical degrees of hepatic PMN infiltration in the presence or absence of the *Il6* gene, indicating that IL-6 is dispensable in this aspect of the inflammatory response. Others have observed that LPS-induced lethality was unaffected by the presence of functional IL-6 (33, 34). Considered together, these data suggest that the role, if any, played by IL-6 in this hepatic PMN infiltration phenotype is subtle or redundant.

Endothelin-1 (*Edn1*) maps close to *D13Mit88*, the marker that showed highly significant linkage at *Hpi1* on Chr 13. *Edn1* is a vasoconstrictor produced by endothelial cells that can act as an autocrine factor to stimulate the production of nitric oxide and prostacyclin, important downstream effectors of the LPS response (35). Further, endotoxemia has been shown to increase hepatic endothelin-1 production (36). This could result in vasoconstriction and ensuing ischemia/reperfusion in the liver, which would exacerbate PMN infiltration and liver damage in B6 mice. Thus, functional allelic differences of *Edn1* in A/J and B6 mice could contribute to the phenotype described here.

Clues to other plausible candidates come from the *Lps*d allele, which encodes a missense mutation in *Tlr4* (11, 12). This component of the LPS signaling pathway is a member of the same gene family as the IL-1 receptor and is also involved in the activation of proinflammatory genes (37, 38). The key role of *Tlr4* in the LPS response illustrates the possibility that mutations affecting elements of the signal transduction cascade initiated by this or other LPS receptors may play important roles in variable response to endotoxemia and, hence, are candidate genes for the phenotype examined here.

In this study, the contribution of the *Hpi1* locus was shown to be epistatic to *Hpi2*. *Hpi2* had no apparent affect on the LPS-induced hepatic PMN infiltration phenotype unless it was homozygous for the B6-type allele in the presence of a homozygous B6 phenotype at *Hpi1*. All intercross mice with B/B genotypes at both *Hpi1* and *Hpi2* had high infiltration scores in response to endotoxin, including most of the highest infiltration scores among the 122 intercross progeny. This prediction held when RI genotypes at *Hpi1* and *Hpi2* were compared to PMN infiltration scores in AXB/BXA RI strains (Fig. 1). The four strains with B/B, B/B genotypes showed 63 ± 14.8 PMN/h.p.f. as compared to 44 ± 12 (A/A, A/A), 37.2 ± (B/B, A/A), and 37.1 ± 9.8 (A/A, B/B). Thus, ascertainment of these two genotypes can identify a subset of mice that will exhibit a strong inflammatory response.

The endotoxin-induced PMN infiltration phenotype seen in mice is directly analogous to the pathology of a number of human diseases characterized by an exaggerated inflammatory response, and therefore the findings of this study have important implications for the management of human patients. A high level of PMN infiltration in response to endotoxin can be predicted based only on a knowledge of genotypes at two loci. Our observations validate such a prediction only in the context of the limited genetic variability between these specific inbred strains. However, these results clearly demonstrate the basis for identifying a larger subset of the repertoire of polymorphic genes that affect predisposition to exaggeration or attenuation of specific aspects of the inflammatory response manifested in mice. Comparative mapping provides a means of extending these observations to human beings, with the possibility that individuals predisposed to an exaggerated inflammatory response could be identified by genetic testing at the time of admission to a surgical intensive care unit, prior to the onset of disease. FJ

Karl Broman suggested methods for evaluating epistatic interactions among *Hpi* loci and for defining QTL candidate regions. Maria Granovsky provided a critical reading of this manuscript. We thank Maria Lourdes Mooney and Joshua Groman for excellent technical assistance and Chris Zink for photography. This work was supported in part by the Robert Garrett Research Foundation (A.D.M.) and by GM57317 (A.D.M. and R.H.R.).

REFERENCES

1. Wenzel, R. (1992) Anti-endotoxin monoclonal antibodies—a second look. *New Engl. J. Med.* **326,** 1151
2. Cerra, F. B. (1987) Hypermetabolism, organ failure, and metabolic support. *Surgery* **101,** 1–14
3. Livingston, D. H., Mosenthal, A. C., and Deitch, E. A. (1995) Sepsis and multiple organ dysfunction syndrome: a clinical-mechanistic overview. *New Horiz.* **3,** 257–266
4. Deitch, E. A. (1992) Multiple organ failure. Pathophysiology and potential future therapy. *Ann. Surg.* **216,** 117–134
5. Zivot, J. B., and Hoffman, W. D. (1995) Pathogenic effects of endotoxin. *New Horiz.* **3,** 267–275
6. Shanley, T. P., Warner, R. L., and Ward, P. A. (1995) The role of cytokines and adhesion molecules in the development of inflammatory injury. *Mol. Med Today* **1,** 40–45
7. Cox, A., and Duff, G. W. (1996) Cytokines as genetic modifying factors in immune and inflammatory diseases. *J. Pediatr. Endocrinol. Metab.* **9** (Suppl. 1), 129–132
8. Sorensen, T. I., Nielsen, G. G., Andersen, P. K., and Teasdale, T. W. (1988) Genetic and environmental influences on premature death in adult adoptees. *N. Engl. J. Med.* **318,** 727–732

9. Stuber, F., Petersen, M., Bokelmann, F., and Schade, U. (1996) A genomic polymorphism within the tumor necrosis factor locus influences plasma tumor necrosis factor-alpha concentrations and outcome of patients with severe sepsis [see comments]. *Crit. Care Med.* **24,** 381–384
10. Fang, X. M., Schroder, S., Hoeft, A., and Stuber, F. (1999) Comparison of two polymorphisms of the interleukin-1 gene family: interleukin-1 receptor antagonist polymorphism contributes to susceptibility to severe sepsis [see comments]. *Crit. Care Med.* **27,** 1330–1334
11. Poltorak, A., He, X., Smirnova, I., Liu, M. Y., Huffel, C. V., Du, X., Birdwell, D., Alejos, E., Silva, M., and Galanos, C. (1998) Defective LPS signaling in C3H/HeJ and C57BL/10ScCr mice: mutations in Tlr4 gene. *Science* **282,** 2085–2088
12. Qureshi, S. T., Lariviere, L., Leveque, G., Clermont, S., Moore, K. J., Gros, P., and Malo, D. (1999) Endotoxin-tolerant Mice Have Mutations in Toll-like Receptor 4 (Tlr4). *J. Exp. Med.* **189,** 615–625
13. De Maio, A., Mooney, M. L., Matesic, L. E., Paidas, C. N., and Reeves, R. H. (1998) Genetic component in the inflammatory response induced by bacterial lipopolysaccharide. *Shock* **10,** 319–323
14. O'Malley, J., Matesic, L. E., Zink, M. C., Strandberg, J. D., Mooney, M. L., De Maio, A., and Reeves, R. H. (1998) Comparison of acute endotoxin-induced lesions in A/J and C57BL/6J mice. *J. Heredity* **89,** 525–30
15. Matesic, L. E., De Maio, A., and Reeves, R. H. (1999) Mapping LPS-response loci in mice using recombinant inbred and congenic strains. *Genomics* **62,** 34–41
16. Thomas, K. R., Deng, C., and Capecchi, M. R. (1992) High-fidelity gene targeting in embryonic stem cells by using sequence replacement vectors. *Mol. Cell. Biol.* **12,** 2919–2923
17. Manly, K. F., and Olson, J. M. (1999) Overview of QTL mapping software and introduction to map manager QT. *Mamm. Genome* **10,** 327–334
18. Sampson, S. B., Higgins, D. C., Elliot, R. W., Taylor, B. A., Lueders, K. K., Koza, R. A., and Paigen, B. (1998) An edited linkage map for the AXB and BXA recombinant inbred mouse strains. *Mamm. Genome* **9,** 688–694
19. Churchill, G. A., and Doerge, R. W. (1994) Empirical threshold values for quantitative trait mapping. *Genetics* **138,** 963–971
20. Lander, E., and Kruglyak, L. (1995) Genetic dissection of complex traits: guidelines for interpreting and reporting linkage results. *Nat. Genet.* **11,** 241–247
21. Kopf, M., Baumann, H., Freer, G., Freudenberg, M., Lamers, M., Kishimoto, T., Zinkernagel, R., Bluethmann, H., and Kohler, G. (1994) Impaired immune and acute-phase responses in interleukin-6-deficient mice. *Nature (London)* **368,** 339–342
22. Vincek, V., Kurimoto, I., Medema, J. P., Prieto, E., and Streilein, J. W. (1993) Tumor necrosis factor alpha polymorphism correlates with deleterious effects of ultraviolet B light on cutaneous immunity. *Cancer Res.* **53,** 728–732
23. Jacob, C. O., Hwang, F., Lewis, G. D., and Stall, A. M. (1991) Tumor necrosis factor alpha in murine systemic lupus erythematosus disease models: implications for genetic predisposition and immune regulation. *Cytokine* **3,** 551–561
24. Nussler, A. K., Wittel, U. A., Nussler, N. C., and Beger, H. G. (1999) Leukocytes, the Janus cells in inflammatory disease. *Langenbecks Arch. Surg.* **384,** 222–232
25. Hewett, J. A., Schultze, A. E., VanCise, S., and Roth, R. A. (1992) Neutrophil depletion protects against liver injury from bacterial endotoxin. *Lab. Invest.* **66,** 347–361
26. Essani, N. A., Fisher, M. A., Farhood, A., Manning, A. M., Smith, C. W., and Jaeschke, H. (1995) Cytokine-induced upregulation of hepatic intercellular adhesion molecule-1 messenger RNA expression and its role in the pathophysiology of murine endotoxin shock and acute liver failure. *Hepatology* **21,** 1632–1639
27. Jaeschke, H., Farhood, A., Fisher, M. A., and Smith, C. W. (1996) Sequestration of neutrophils in the hepatic vasculature during endotoxemia is independent of beta 2 integrins and intercellular adhesion molecule-1. *Shock* **6,** 351–356
28. Mochida, S., Ohno, A., Arai, M., Tamatani, T., Miyasaka, M., and Fujiwara, K. (1996) Role of adhesion molecules in the development of massive hepatic necrosis in rats. *Hepatology* **23,** 320–328
29. Pearson, J. M., Bailie, M. B., Fink, G. D., and Roth, R. A. (1997) Neither platelet activating factor nor leukotrienes are critical mediators of liver injury after lipopolysaccharide administration. *Toxicology* **121,** 181–189
30. Hierholzer, C., Kalff, J. C., Omert, L., Tsukada, K., Loeffert, J. E., Watkins, S. C., Billiar, T. R., and Tweardy, D. J. (1998) Interleukin-6 production in hemorrhagic shock is accompanied by neutrophil recruitment and lung injury. *Am. J. Physiol.* **275,** L611–L621
31. Hoekzema, R., Verhagen, C., van Haren, M., and Kijlstra, A. (1992) Endotoxin-induced uveitis in the rat. The significance of intraocular interleukin-6. *Invest. Ophthalmol. Vis. Sci.* **33,** 532–539
32. Rosenbloom, A. J., Pinsky, M. R., Bryant, J. L., Shin, A., Tran, T., and Whiteside, T. (1995) Leukocyte activation in the peripheral blood of patients with cirrhosis of the liver and SIRS. Correlation with serum interleukin-6 levels and organ dysfunction. *J. Am. Med. Assoc.* **274,** 58–65
33. Fattori, E., Cappelletti, M., Costa, P., Sellitto, C., Cantoni, L., Carelli, M., Faggioni, R., Fantuzzi, G., Ghezzi, P., and Poli, V. (1994) Defective inflammatory response in interleukin 6-deficient mice. *J. Exp. Med.* **180,** 1243–1250
34. Bucklin, S. E., Silverstein, R., and Morrison, D. C. (1993) An interleukin-6-induced acute-phase response does not confer protection against lipopolysaccharide lethality. *Infect. Immun.* **61,** 3184–3189
35. Maemura, K., Kurihara, H., Kurihara, Y., Nagai, R., and Yazaki, Y. (1994) Isolation and characterization of vascular endothelial cells derived from mice lacking endothelin-1. *Biochem. Biophys. Res. Commun.* **201,** 538–545
36. Eakes, A. T., Howard, K. M., Miller, J. E., and Olson, M. S. (1997) Endothelin-1 production by hepatic endothelial cells: characterization and augmentation by endotoxin exposure. *Am. J. Physiol.* **272,** G605—G611
37. Medzhitov, R., Preston-Hurlburt, P., and Janeway, C. A., Jr. (1997) A human homologue of the *Drosophila* toll protein signals activation of adaptive immunity [see comments]. *Nature (London)* **388,** 394–397
38. Rock, F. L., Hardiman, G., Timans, J. C., Kastelein, R. A., and Bazan, J. F. (1998) A family of human receptors structurally related to *Drosophila* toll. *Proc. Natl. Acad. Sci. USA* **95,** 588–593

Received for publication January 3, 2000.
Revised for publication April 28, 2000.